ACS OMEGA

http://pubs.acs.org/journal/acsodf

Article

Antioxidant and Neuroprotective Xenicane Diterpenes from the Brown Alga *Dictyota coriacea*

Yu Qi,▽ Ge Liu,▽ Chengyan Fang,▽ Chengcheng Jing, Shuhua Tang, Ge Li, Chaojie Wang, Haoru Zhu, Min Zhao, Zhongmin Sun, Jianzhang Wu,* and Pengcheng Yan*

Cite This: *ACS Omega* 2023, 8, 8034−8044

Read Online

ACCESS | Metrics & More | Article Recommendations | Supporting Information

ABSTRACT: Five new xenicane diterpenes, including three rare nitrogen-containing derivatives, dictyolactams A (**1**) and B (**2**) and 9-demethoxy-9-ethoxyjoalin (**3**), a rare diterpene with a cyclobutanone moiety, named 4-hydroxyisoacetylcoriacenone (**4**), and 19-*O*-acetyldictyodiol (**5**), were isolated from an East China Sea collection of the brown alga *Dictyota coriacea*, along with 15 known analogues (**6**−**20**). The structures of the new diterpenes were elucidated by spectroscopic analyses and theoretical ECD calculations. All compounds had cytoprotective effects against oxidative stress in neuron-like PC12 cells. The antioxidant mechanism of 18-acetoxy-6,7-epoxy-4-hydroxydictyo-19-al (**6**) was related to the activation of Nrf2/ARE signaling pathway; it also showed significant neuroprotective effects against cerebral ischemia-reperfusion injury (CIRI) *in vivo*. This study provided xenicane diterpene as a promising lead scaffold for the development of potent neuroprotective agents against CIRI.

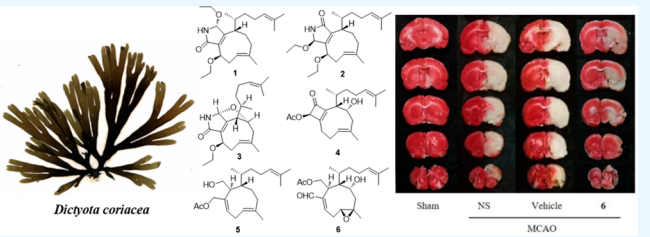

Oxidative stress is considered to be one of the key pathogenic factors contributing to the occurrence and development of neurological diseases, especially cerebral ischemia-reperfusion injury (CIRI) brought about by thrombolytic therapy for ischemic stroke.[1] Nrf2/ARE signaling pathway is the most important endogenous defense system protecting nerve cells against oxidative damage.[2] Some natural products derived from terrestrial plants, such as britanin,[3] swertiamain,[4] and dl-3-*n*-butylphthalide,[5] have proven to be able to prevent and mitigate CIRI by activating Nrf2 and enhancing antioxidant gene expression in the preclinical studies. However, the potential of marine natural products as novel neuroprotective antioxidants against CIRI has been rarely studied yet.[6]

Marine brown algae of the genus *Dictyota* (family Dictyotacea) are a rich source of diterpenes with diverse scaffolds,[7] many of which are biologically active (cytotoxic, antibacterial, antiviral, and antioxidant properties[6,8−14]). Previously, we reported the structure elucidation of dictyospiromide, a unique spirosuccinimide alkaloid with antioxidant properties that are associated with the activation of the Nrf2/ARE signaling pathway from the EtOAc extract of *D. coriacea*.[15] Further chemical investigation of this species led to the isolation of 20 xenicane diterpene derivatives (**1**−**20**) including five new compounds (**1**−**5**), three of which contain a γ-lactam moiety (**1**−**3**) (Chart 1). These diterpenes were tested for their protective activities against oxidative stress in neuron-like PC12 cells; one of the major components **6** was selected for detailed studies of the antioxidant mechanism of action *in vitro* and the neuroprotective effect against CIRI *in vivo*. The details of isolation, structure elucidation, and biological evaluations of these xenicane diterpenes are described below.

RESULTS AND DISCUSSION

Sequential column chromatography of the EtOAc extract of the brown alga *D. coriacea* yielded 20 xenicane diterpenes (**1**−**20**) including five new compounds (**1**−**5**) (Chart 1). The structures were established by 1D and 2D NMR (HSQC, HMBC, COSY, NOESY), HRESIMS, IR, and ECD spectroscopic and spectrometric analyses. Fifteen known compounds were identified as 18-acetoxy-6,7-epoxy-4-hydroxydictyo-19-al (**6**),[16] 18-acetoxy-4-hydroxydictyo-19-al (**7**),[17] 6,7-epoxy-4-hydroxydictyolactone (**8**),[18] 18-hydroxydictyolactone (**9**),[19] 4-hydroxydictyolactone (**10**),[20] (2*S**,3*S**,4*R**,10*R**,19*R**)-19-deoxo-4-hydroxy-19-methoxydictyolactone (**11**),[8] (2*S**,3*S**,4*R**,10*R**,19*S**)-19-deoxo-4-hydroxy-19-methoxydictyolactone (**12**),[8] isodictyohemiacetal (**13**),[17] 4-hydroxycrenulide (**14**),[21] 4,18-dihydroxycrenulide (**15**),[22] 4-acetoxycrenulide (**16**),[22] 18-hydroxy-4-acetoxycrenulide (**17**),[22] crenulacetal B (**18**),[23] 4-hydroxypachylactone (**19**),[13] and 4-acetoxysanadaol (**20**)[24] by comparing their ^{1}H and ^{13}C NMR

Received: December 11, 2022
Accepted: February 7, 2023
Published: February 16, 2023

Chart 1. Chemical Structures of the Xenicane Diterpenes 1−20

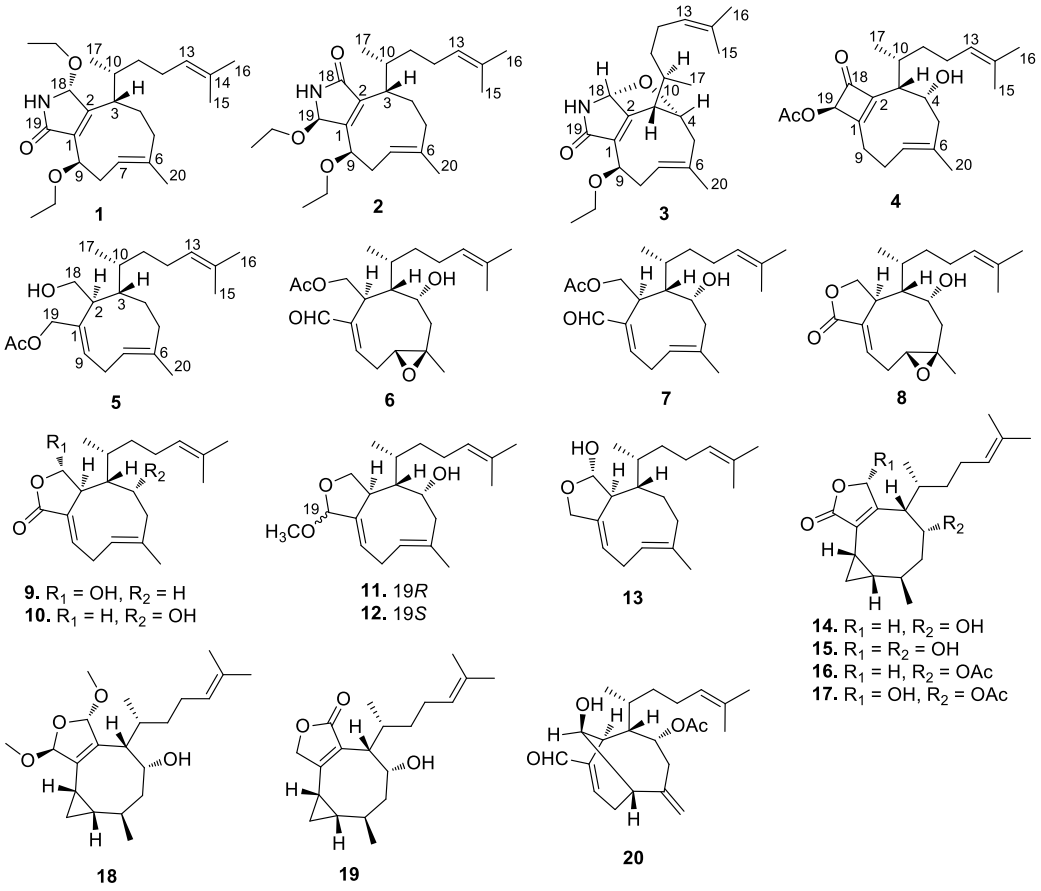

and MS data, as well as specific rotations with those reported in the literature.

Compound **1** had a molecular formula of $C_{24}H_{39}NO_3$ as determined by HRESIMS data, requiring six degrees of unsaturation. The IR absorptions at 3273 and 1697 cm^{-1} indicated the presence of amino and carbonyl groups. The ^1H NMR spectrum of **1** displayed three methyl singlets at δ_H 1.62 (s, H_3-16), 1.57 (s, H_3-15), 1.24 (s, H_3-20), a methyl doublet at δ_H 0.98 (d, J = 6.0 Hz, H_3-17), and two methyl triplets at δ_H 1.22 (t, J = 7.2 Hz) and 1.15 (t, J = 7.2 Hz) that attributed to two ethoxy groups (Table 1). The ^{13}C NMR spectrum showed 24 carbon signals including a carbonyl (δ_C 172.7, C-19) and six olefinic carbons at δ_C 160.5 (C, C-2), 140.8 (C, C-6), 133.4 (C, C-1), 130.7 (C, C-14), 126.1 (CH, C-13), and 121.6 (CH, C-7) (Table 2), which accounted for four of the six degrees of unsaturation. Thus, **1** must be bicyclic. A γ-ethoxy-α,β-unsaturated-γ-lactam moiety was easily recognized by COSY correlations between an NH (δ_H 7.63, br s) and a heteroacetal proton H-18 (δ_H 5.41, d, J = 1.2 Hz) and between an oxygenated methylene (δ_H 3.76, m; 3.61, m) and a methyl triplet (δ_H 1.22, t, J = 7.2 Hz), as well as HMBC correlations from NH and H-18 to the two olefinic nonprotonated carbons C-1 and C-2, from H-18 to the carbonyl carbon C-19, and from the oxygenated methylene protons to a methine carbon C-18 (δ_C 85.6, CH) (Figure 1). COSY correlations of H-3 (δ_H 2.65, t, J = 9.0 Hz)/H_2-4 (δ_H 2.10, m; 1.95, m), H_2-4/H_2-5 (δ_H 2.19, m; 1.96, m), H-7 (δ_H 5.36, dd, J = 12.6, 4.2 Hz)/H_2-8 (δ_H 2.45, dt, J = 13.2, 4.2 Hz; 1.86, td, J = 13.2, 2.4 Hz), and H_2-8/H-9 (δ_H 4.64, dd, J = 4.2, 2.4 Hz) defined two proton spin systems. HMBC correlations from the olefinic methyl H_3-20 to an aliphatic methylene carbon C-5 (δ_C 41.4, CH_2) and two olefinic carbons C-6 and C-7 and from H-3 and H-9 to two olefinic carbons C-1 and C-2 allowed the construction of a nine-membered ring, in which C-1 and C-2 were also constituents of the α,β-unsaturated-γ-lactam, C-6/C-7 composed a double bond, C-6 was substituted by a methyl group, and C-9 (δ_C 77.4, CH) was oxygenated. In addition, the fusion of the ring system was revealed by HMBC correlations from H-9 to the carbonyl carbon C-19 and from H-3 to the methine carbon C-18. Moreover, a 6-methylhept-5-en-2-yl side chain was established by COSY correlations of H-13 (δ_H 5.08, t, J = 7.2 Hz)/H_2-12 (δ_H 2.04, m; 1.83, m), H_2-12/H_2-11 (δ_H 1.65, m; 0.86, m), H_2-11/H-10 (δ_H 1.84, m), and H-10/H_3-17, as well as HMBC correlations from two olefinic methyls H_3-15 and H_3-16 to two olefinic carbons C-13 and C-14 and from H_3-17 to an aliphatic methine carbon C-10 (δ_C 35.5, CH) and an aliphatic methylene carbon C-11 (δ_C 36.8, CH_2). All these NMR data are characteristic of a xenicane-type diterpene represented by the co-occurring analogues 18-hydroxydictyolactone (**9**)[19] and 4-hydroxydictyolactone (**10**).[20] The side chain was connected to the nine-membered ring via C-3 by COSY correlation between H-3 and H-10 and HMBC correlation from H_3-17 to C-3, while the second ethoxy group was attached to C-9 according to COSY correlations between the oxygenated methylene protons (δ_H 3.49, m; 3.43, m) and the methyl triplet at δ_H 1.15 (t, J = 7.2 Hz) and HMBC correlations from the oxygenated methylene protons to the oxygenated methine carbon C-9. Thus, the planar structure of

https://doi.org/10.1021/acsomega.2c07891
ACS Omega 2023, 8, 8034−8044

Table 1. ^{1}H NMR Spectroscopic Data for 1−5 (Acetone-d_6)[a]

no.	1[b]	2[c]	3[c]	4[c]	5[c]
2					2.72, dd (9.5, 6.0)
3	2.65, t (9.0)	2.36, t (9.5)	2.78, d (10.5)	2.14, d (10.0)	1.72, d (9.5)
4	2.10, m	2.33, m	4.67, dd (3.0, 1.5)	4.55, br s	1.69, m
	1.95, m	1.90, m			1.56, m
5	2.19, m	2.13, m	2.32, dd (13.0, 3.5)	2.35, m	2.23, br d (12.0)
	1.96, m	1.96, m	2.15, br d (13.0)	2.17, m	1.95, m
7	5.36, dd (12.6, 4.2)	5.40, dd (12.5, 3.5)	5.36, br d (10.5)	5.27, dd (10.0, 4.5)	5.44, br d (12.0)
8	2.45, dt (13.2, 4.2)	2.49, dt (13.5, 4.0)	2.50, dt (13.0, 3.0)	2.69, m	3.04, t (13.5)
	1.86, td (13.2, 2.4)	2.12, m	2.20, td (13.0, 3.0)	2.32, m	2.57, dd (13.5, 8.5)
9	4.64, dd (4.2, 2.4)	4.37, dd (4.0, 2.5)	4.54, br t (2.5)	2.30, m	5.77, br d (9.0)
				2.27, m	
10	1.84, m	2.02, m	1.78, m	2.16, m	1.83, m
11	1.65, m	1.35, m	1.52, m	1.38, m	1.26, dd (15.0, 9.0)
	0.86, m	0.91, m	1.17, m	1.10, m	
12	2.04, m	2.04, m	2.11, m	1.93, m	2.00, m
	1.83, m	1.81, m	1.96, m	1.87, m	
13	5.08, t (7.2)	5.03, t (7.0)	5.08, t (6.5)	5.06, t (7.0)	5.13, t (7.0)
15	1.57, s	1.55, s	1.58, s	1.56, s	1.62, s
16	1.62, s	1.61, s	1.65, s	1.64, s	1.68, s
17	0.98, d (6.0)	0.96, d (6.5)	1.05, d (6.5)	0.99, d (6.5)	0.86, d (6.5)
18	5.41, d (1.2)		5.63, br s		3.80, dd (10.0, 6.0)
					3.61, t (10.0)
19		5.07, d (2.0)		5.93, s	4.58, dt (13.0, 1.5)
					4.53, dt (13.0, 1.5)
20	1.24, s	1.26, s	1.56, s	1.55, s	1.75, s
9-OEt	3.49, m	3.53, m	3.51, m		
	3.43, m	3.45, m	1.17, t (7.0)		
	1.15, t (7.2)	1.15, t (7.0)			
18/19-OEt	3.76, m	3.52, m			
	3.61, m	3.50, m			
	1.22, t (7.2)	1.16, t (7.0)			
OAc				2.04, s	2.04, s
NH/OH	7.63, br s	7.43, br s	7.39, br s	3.72, br s	

[a]The coupling constants (J) are in parentheses and reported in Hz; chemical shifts are given in ppm. [b]600 MHz. [c]500 MHz.

1 was elucidated as 9,18-diethoxyxenica-1,6,13-trien-19,18-lactam.

The relative configuration of **1** was determined by coupling constant and NOE analysis. The coupling pattern of H-3 (δ_H 2.65, t, J = 9.0 Hz) indicated the *anti* orientations of H-3/H-4b (δ_H 1.95, m) and H-3/H-10 (δ_H 1.84, m). The *E* geometry of the C-6/C-7 double bond was suggested by the diagnostic chemical shift of C-20 (<20 ppm)[25,26] and confirmed by NOE correlations of H-7/H-5b (δ_H 1.96, m) and H_3-20/H-8b (δ_H 1.86, td, J = 13.2, 2.4 Hz) (Figure 2). NOE correlations of H-7/H-3, H-3/H_3-17, and H-4a (δ_H 2.10, m)/H_3-17 suggested the 3*S**,10*R** assignment, while the small coupling constant values of $J_{H\text{-}9/H\text{-}8a}$ (4.2 Hz) and $J_{H\text{-}9/H\text{-}8b}$ (2.4 Hz) indicated the *gauche* orientations of H-9/H-8a (δ_H 2.45, dt, J = 13.2, 4.2 Hz) and H-9/H-8b, requiring the 9*R** configuration. The relative configuration of C-18 cannot be determined by NOE correlations. The absolute configuration at C-18 was established by the application of the electronic circular dichroism (ECD) helicity rule originally used for α,β-unsaturated-γ-lactones.[27] The negative Cotton effect at 217 nm ($\pi-\pi^*$ transition) in the ECD spectrum was consistent with the anticlockwise screw. Therefore, the absolute configuration at C-18 was assigned as *R*. In addition, the absolute configurations of 3*S*,10*R* were determined to be in agreement with those of 4-hydroxydictyolactone (**10**)[20] by biogenetic considerations. This assignment was further supported by the calculated ECD data of **1** at the B3LYP/Def2-TZVP level (Figure S36), which showed a similar ECD curve as that of the experimental ECD spectrum. Compound **1** was given the name dictyolactam A. The ethyl ether is possibly an artifact because EtOH was used during the extraction process; however no evidence of the nonetherified form of **1** was observed during the isolation procedure. In either case, the free hydroxy or ethyl ether form of **1** is the second natural nitrogen-containing xenicane diterpene.[28]

Compound **2** had the same molecular formula as that of **1** according to its HRESIMS data. It was revealed to be an isomer of **1** with respect to the α,β-unsaturated-γ-lactam ring by extensive 2D NMR spectroscopic analysis and comparison of the NMR data with those of **1** (Tables 1 and 2). HMBC correlations from H-3 (δ_H 2.36, t, J = 9.5 Hz) to a carbonyl carbon C-18 (δ_C 173.0, C) and from the heteroacetal proton H-19 (δ_H 5.07, d, J = 2.0 Hz) to an oxygenated methine carbon C-9 (δ_C 78.0, CH), the carbonyl carbon C-18, and two olefinic nonprotonated carbons C-1 (δ_C 150.9, C) and C-2 (δ_C 142.6, C) disclosed that the fusion of the α,β-unsaturated-γ-lactam ring was reversed in **2** (Figure 1). The relative configurations at C-3, C-9, and C-10 and the geometry of the C-6/C-7 double bond were suggested to be the same as those of **1** based on the similar coupling constants and NOE relationships (Figure 2).

https://doi.org/10.1021/acsomega.2c07891
ACS Omega 2023, 8, 8034−8044

Table 2. ^{13}C NMR Data for 1−5 (Acetone-d_6)[a]

no.	1[b]	2[c]	3[c]	4[c]	5[c]
1	133.4, C	150.9, C	132.8, C	173.2, C	144.1, C
2	160.5, C	142.6, C	162.6, C	160.5, C	47.8, CH
3	47.1, CH	44.9, CH	50.5, CH	49.0, CH	48.4, CH
4	35.8, CH_2	34.3, CH_2	94.5, CH	78.2, CH	28.9, CH_2
5	41.4, CH_2	41.7, CH_2	45.6, CH_2	49.1, CH_2	42.1, CH_2
6	140.8, C	141.6, C	140.5, C	140.1, C	135.6, C
7	121.6, CH	120.5, CH	121.7, CH	125.8, CH	126.6, CH
8	30.7, CH_2	30.7, CH_2	32.5, CH_2	27.9, CH_2	28.4, CH_2
9	77.4, CH	78.0, CH	78.5, CH	24.4, CH_2	129.0, CH
10	35.5, CH	35.2, CH	35.5, CH	32.3, CH	33.8, CH
11	36.8, CH_2	36.5, CH_2	36.4, CH_2	35.9, CH_2	39.2, CH_2
12	27.2, CH_2	26.7, CH_2	26.5, CH_2	25.5, CH_2	26.9, CH_2
13	126.1, CH	125.9, CH	125.3, CH	125.5, CH	125.8, CH
14	130.7, C	131.1, C	131.9, C	131.6, C	131.6, C
15	17.7, CH_3	17.7, CH_3	17.7, CH_3	17.7, CH_3	17.8, CH_3
16	25.8, CH_3	25.8, CH_3	25.8, CH_3	25.9, CH_3	25.8, CH_3
17	18.7, CH_3	18.7, CH_3	18.5, CH_3	18.1, CH_3	16.9, CH_3
18	85.6, CH	173.0, C	86.8, CH	186.6, C	60.7, CH_2
19	172.7, C	84.3, CH	174.8, C	83.9, CH	66.7, CH_2
20	15.8, CH_3	15.9, CH_3	20.1, CH_3	19.4, CH_3	17.5, CH_3
9-OEt	65.2, CH_2	65.1, CH_2	65.4, CH_2		
	15.8, CH_3	15.8, CH_3	15.7, CH_3		
18/19-OEt	65.8, CH_2	61.1, CH_2			
	15.8, CH_3	15.8, CH_3			
OAc				170.6, C	170.7, C
				20.7, CH_3	21.0, CH_3

[a]The assignments were based on HSQC, HMBC, and COSY spectra. [b]150 MHz. [c]125 MHz.

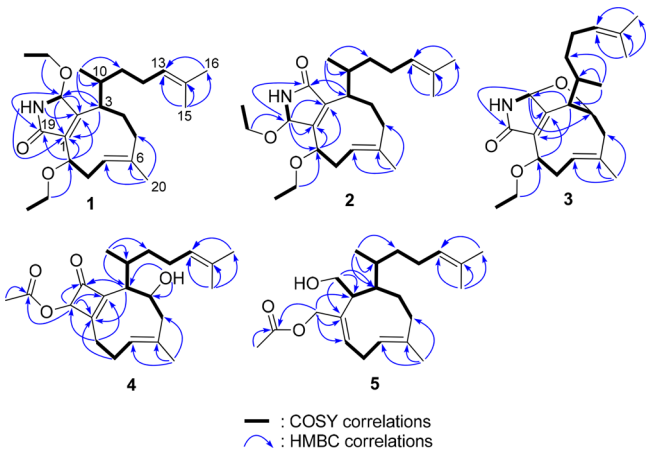

Figure 1. Key COSY and HMBC correlations for 1−5.

The NOE correlation between H-19 and H-8b (δ_H 2.12, m) indicated the 19*R** configuration. The experimental ECD spectrum of **2** was similar to that of **1** (Figure S36), implying the same absolute configuration at the heteroacetal carbons. This was supported by the overall match of the experimental and calculated ECD curves for **2**. It was given the name dictyolactam B.

The NMR data of **3** were comparable to those of joalin,[28] the first nitrogen-containing xenicane from the genus *Dictyota*, with the exception of additional signals for an ethoxy [δ_H 3.51 (m), 1.17 (t, J = 7.0 Hz); δ_C 65.4 (CH_2), 15.7 (CH_3)] and loss of signals for a methoxy group (Tables 1 and 2), indicating that **3** was an ethoxylated 9-demethoxyjoalin. The ethoxy group was attached to C-9 (δ_C 78.5, CH) by HMBC correlations from the oxygenated methylene protons to an oxygenated methine carbon C-9 (Figure 1). The relative configuration of **3** was suggested to be in agreement with that of joalin[28] by NOE correlations of H-3 (δ_H 2.78, d, J = 10.5 Hz)/H-7 (δ_H 5.36, br d, J = 10.5 Hz), H-7/H-5b (δ_H 2.15, br d, J = 13.0 Hz), H-4 (δ_H 4.67, dd, J = 3.0, 1.5 Hz)/H-18 (δ_H 5.63, br s), H-18/H-10 (δ_H 1.78, m), and H-4/H_3-17 (δ_H 1.05, d, J = 6.5 Hz) (Figure 2) and similar coupling constant values $J_{H\text{-}3/H\text{-}10}$ (10.5 Hz, **3**; 10.3 Hz, joalin), $J_{H\text{-}4/H\text{-}5}$ (3.5, 1.5 Hz, **3**; 3.6, 2.2 Hz, joalin), and $J_{H\text{-}8/H\text{-}9}$ (2.5 Hz, **3**; 3.1 Hz, joalin). The absolute configuration 3*S*,4*R*,9*R*,10*R*,18*R* was assigned based on the high similarity between the measured and calculated ECD spectra for **3** (Figure S36). Thus, compound **3** was established as 9-demethoxy-9-ethoxyjoalin.

The molecular formula of compound **4** was determined to be $C_{22}H_{32}O_4$ by its HRESIMS data. The ^{1}H and ^{13}C NMR data of **4** closely paralleled those of previously reported xenicane diterpenes with a cyclobutanone moiety, acetylcoriacenone and isoacetylcoriacenone,[29] except for the loss of signals for an aliphatic methylene and the appearance of additional signals for a secondary alcohol [δ_H 4.55 (br s, H-4), 3.72 (br s, OH); δ_C 78.2 (CH, C-4)] (Tables 1 and 2), indicating that **4** was a hydroxylated derivative of acetylcoriacenone or isoacetylcoriacenone. This assumption was supported by the additional oxygen relative to the molecular formula of these two xenicanes. The location of the secondary alcohol was assigned at C-4 based on the HMBC correlation from the 4-OH proton to an aliphatic methine carbon C-3 (δ_C 49.0, CH), along with COSY correlations between the oxygenated methine proton H-4/H-3 (δ_H 2.14, d, J = 10.0 Hz) and H-4/H_2-5 (δ_H 2.35, m; 2.17, m) (Figure 1). The configurations at the C-3, C-10, and C-6/C-7 double bonds (3*S**,10*R**,6*E*) were assigned as in agreement with those of acetylcoriacenone and isoacetylcoriacenone[29] based on biogenetic considerations and the similar NMR data, including the large coupling constant value $J_{H\text{-}3/H\text{-}10}$ (10.0 Hz, indicating the *anti* orientations of H-3/H-10) and NOE correlations of H-3/H-7 (δ_H 5.27, dd, J = 10.0, 4.5 Hz) and H-7/H-5b (δ_H 2.17, m) (Figure 2). The broad singlet observed for H-4 (weak vicinal coupling between H-3 and H-4) suggested an H3−C3−C4−H4 dihedral angle value of approximately 90°, requiring the 4*R** configuration. This was supported by the NOE correlation between H-4 and H_3-17 (δ_H 0.99, d, J = 6.5 Hz). In addition, the NOE correlations between H-19 (δ_H 5.93, s) and H_3-20 (δ_H 1.55, s) revealed the 19*R** configuration. The absolute configuration at C-19 was determined to be the same as that of isoaceylcoriacenone[29] by the similar measured ECD curves and confirmed by the calculated ECD curve for 19*R*-enantiomer of **4** (Figure S36). Therefore, **4** was defined as 4-hydroxyisoacetylcoriacenone.

The ^{1}H and ^{13}C NMR data recorded for **5** were comparable to those of dictyodiol,[30] except for the appearance of additional signals attributed to an acetyl group [δ_H 2.04 (s); δ_C 170.7 (C), 21.0 (CH_3)] (Tables 1 and 2), indicating that **5** was an acetylated derivative of dictyodiol. The acetoxy group was located at C-19 (δ_C 66.7, CH_2), as supported by HMBC correlations from the oxygenated methylene H_2-19 (δ_H 4.58, dt, J = 13.0, 1.5 Hz; 4.53, dt, J = 13.0, 1.5 Hz) to the carbonyl carbon, two olefinic carbons C-1 (δ_C 144.1, C) and C-9 (δ_C 129.0, CH), and an aliphatic methine carbon C-2 (δ_C 47.8, CH) (Figure 1). The relative configuration of **5** was suggested to be the same as that of dictyodiol[30] based on the similar weak

https://doi.org/10.1021/acsomega.2c07891
ACS Omega 2023, 8, 8034−8044

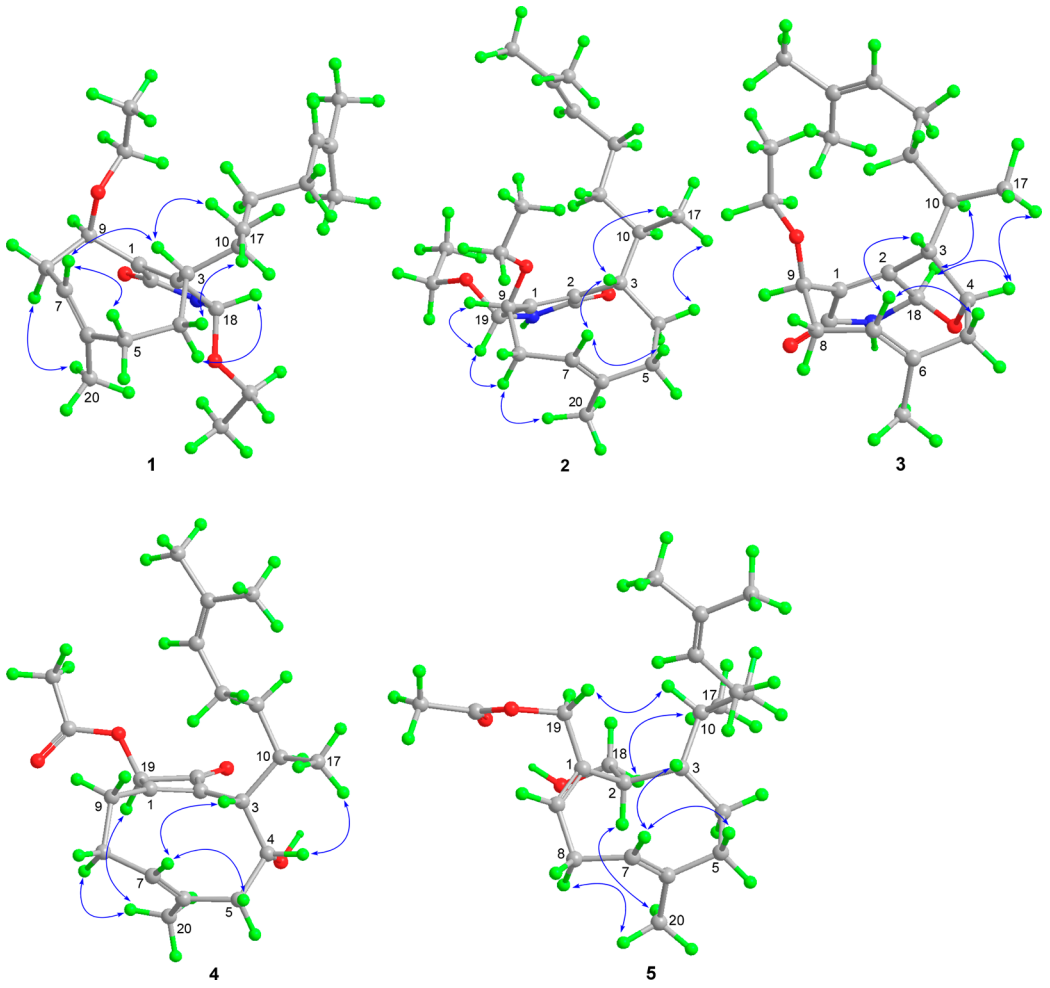

Figure 2. Key NOE correlations for **1**−**5**.

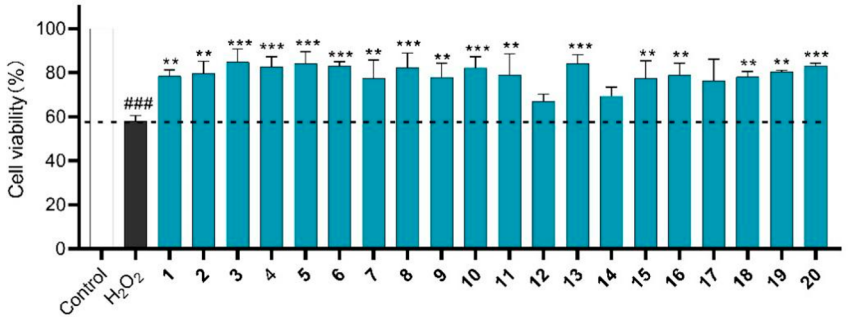

Figure 3. Cytoprotection of **1**−**20** against H_2O_2-induced oxidative damage in PC12 cells. PC12 cells were pretreated with 2 μM concentrations of compounds for 6 h and then cocultured with 500 μM of H_2O_2 for 24 h. The cell viability was determined by the MTT assay. Data are expressed as the mean ± SD, n = 3. $^{\#\#\#\#}P < 0.0001$ vs control; $^{***}P < 0.001$, $^{**}P < 0.01$ vs H_2O_2.

vicinal couplings between H-2 (δ_H 2.72, dd, J = 9.5, 6.0 Hz)/H-3 (δ_H 1.72, d, J = 9.5 Hz) and H-3/H-10 (δ_H 1.83, m) (indicating the H2−C2−C3−H3 and H3−C3−C10−H10 dihedral angle values of approximately 90°), in combination with significant NOE correlations of H-2/H_3-20 (δ_H 1.75, s), H-3/H-7 (δ_H 5.44, br d, J = 12.0 Hz), H_2-18 (δ_H 3.80, dd, J = 10.0, 6.0 Hz; 3.61, t, J = 10.0 Hz)/H_3-17 (δ_H 0.86, d, J = 6.5 Hz), and H_2-19/H-10 (Figure 2). Thus, compound **5** was determined as 19-*O*-acetyldictyodiol.

All of the xenicane diterpenes **1**−**20** were evaluated for their cytoprotective effects against hydrogen peroxide (H_2O_2)-induced oxidative damage in neuron-like pheochromocytoma PC12 cells by the MTT method.[31,32] As shown in Figure 3, the cell survival rate of PC12 cells treated with H_2O_2 was around 57% compared with the control group, and it was increased to 77%−84% by treatments with 2 μM **1**−**11**, **13**,**15**, **16**, and **18**−**20**, while **12**, **14**, and **17** showed weaker cytoprotection than the other analogues in this assay.

Compound **6**, a major active component of this alga, probably had higher water solubility comparing with the other analogues due to its highly oxygenated nature. It was thus selected for further studies to investigate the antioxidant

https://doi.org/10.1021/acsomega.2c07891
ACS Omega 2023, 8, 8034−8044

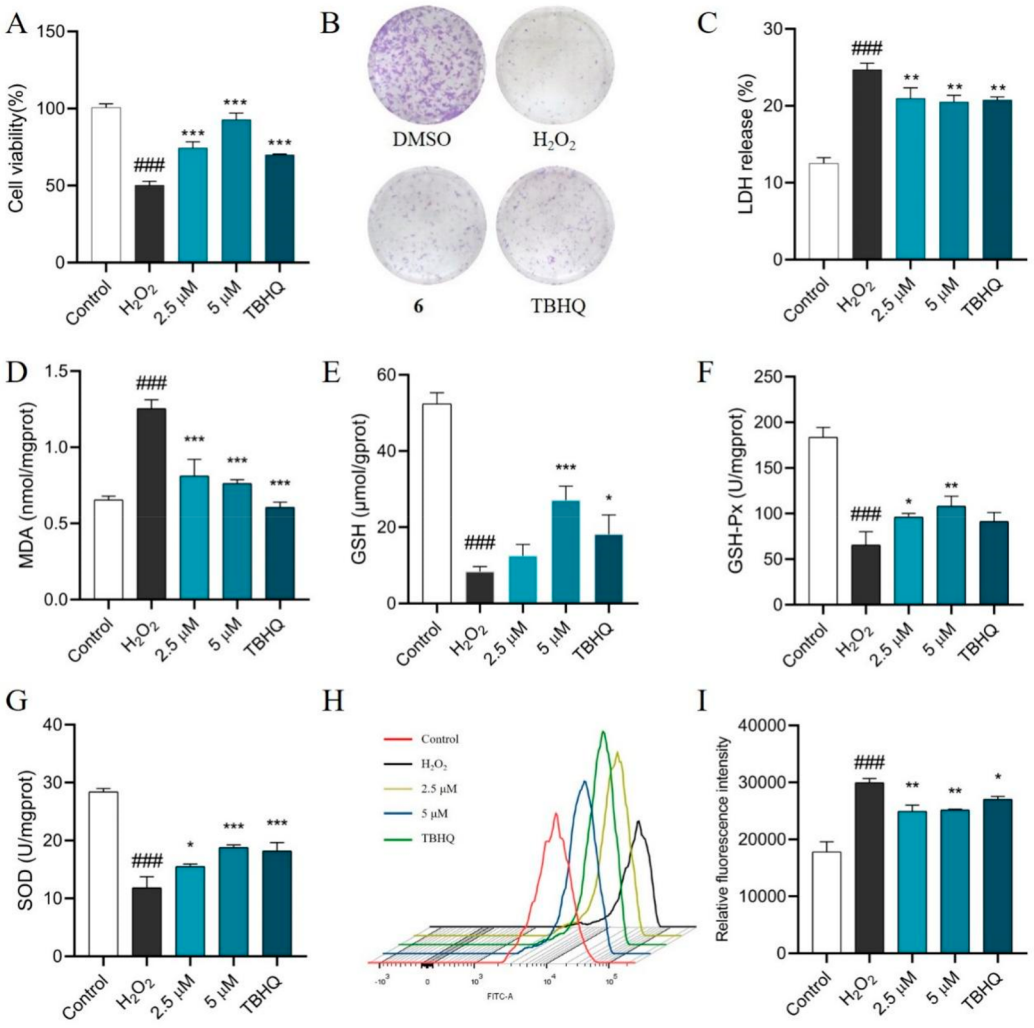

Figure 4. Protective effect of **6** against H_2O_2-induced oxidative damage in PC12 cells. (A) **6** increased cell survival rate in a H_2O_2 damage model. (B) Pretreatment with 5 μM **6** promoted colony formation. (C, D) **6** decreased the levels of LDH and MDA, respectively. (E−G) **6** increased the levels of GSH, GSH-Px, and SOD, respectively. (H, I) **6** inhibited the excessive production of intracellular ROS stimulated by H_2O_2 in PC12 cells. ROS levels were detected using flow cytometry. PC12 cells were preincubated with **6** for 6 h prior to another 24 h exposure to 500 μM H_2O_2. TBHQ (10 μM) was used as a positive control. Data are expressed as the mean ± SD, $n = 3$. $^{\#\#\#}P < 0.001$ vs control; $^{***}P < 0.001$, $^{**}P < 0.01$, $^{*}P < 0.05$ vs H_2O_2.

properties of xenicane diterpenes. It showed no cytotoxic activity toward PC12 cells at the concentration of 5 μM in the MTT assay (Figure S68). Thus, the maximum concentration of **6** was set as 5 μM in the following antioxidant evaluations in PC12 cells. As shown in Figure 4A, the viability of PC12 cells injured by H_2O_2 was significantly increased by **6** (2.5 and 5 μM), and the cytoprotection of **6** (2.5 μM) was comparable to that of the positive control *tert*-butylhydroquinone (TBHQ, 10 μM). The cytoprotection of **6** was confirmed by a colony formation assay.[32,33] Compound **6** (5 μM) significantly promoted colony formation of PC12 cells treated by H_2O_2 with the effect comparable to that of the positive control TBHQ (10 μM) (Figure 4B). In addition, **6** (2.5 and 5 μM) could significantly reduce the lactate dehydrogenase (LDH) level (which correlates with the number of dead cells[34]) released by PC12 cells treated with H_2O_2 (Figure 4C), indicating a potent cytoprotective effect against oxidative damage in PC12 cells.

The antioxidant property of **6** was further evaluated using the malondialdehyde (MDA), glutathione (GSH), glutathione peroxide (GSH-Px), and superoxide dismutase (SOD) assay kits in the H_2O_2-induced PC12 cell damage model. As shown in Figure 4D−G, 6 h of pretreatment with **6** significantly inhibited the MDA production and upregulated the levels of GSH, GSH-Px, and SOD in a dose-dependent manner. In addition, pretreatment with **6** significantly reduced the intracellular ROS production induced by H_2O_2 based on the dichlorodihydrofluorescein diacetate (DCFH-DA) assay[32] (Figure 4H, I). Overall, **6** has potent antioxidant and cytoprotective activities in PC12 cells.

Compound **6** was tested for the free radical scavenging capacity using a DPPH (2,2-diphenyl-1-picrylhydrazyl) assay.[3] It showed no scavenging effect even at a high concentration of 20 μM (Figure S69), indicating an indirect antioxidant that cannot remove excessive ROS via chemical ways. Compound **6** was also detected for the activation of the Nrf2/ARE, a key signaling pathway in the antioxidant defense response.[2] As shown in Figure 5A−C, **6** upregulated the levels of Nrf2 and heme oxygenase-1 (HO-1), an antioxidant protein regulated by Nrf2,[35] in a dose-dependent manner based on a Western-blot

https://doi.org/10.1021/acsomega.2c07891
ACS Omega 2023, 8, 8034−8044

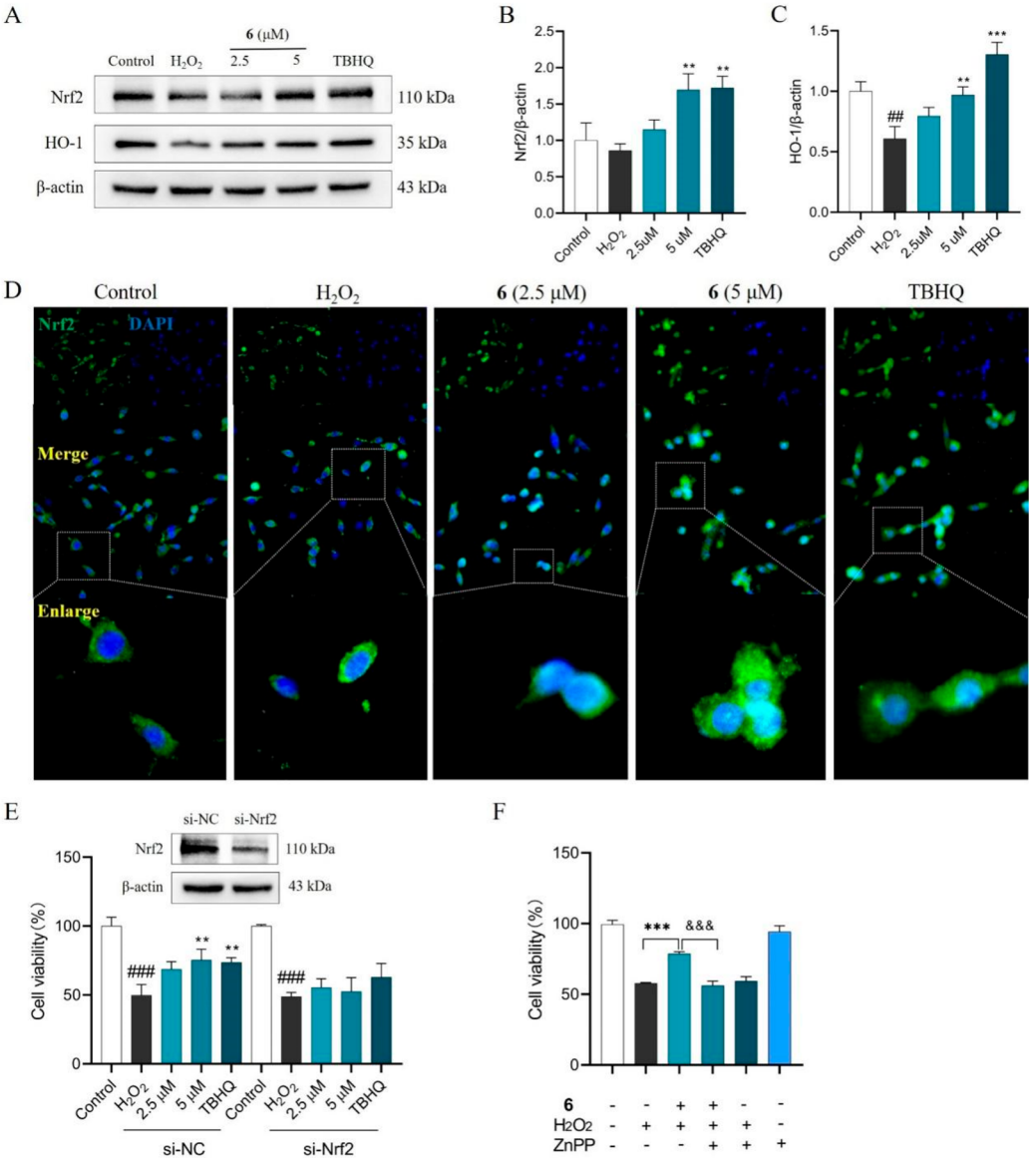

Figure 5. Compound **6** exerts antioxidant effect in PC12 cells by activating the Nrf2/ARE pathway. (A–C) **6** increased the expressions of Nrf2 and HO-1 proteins. The Nrf2 and HO-1 protein levels were determined by Western blotting. (D) **6** induced Nrf2 nuclear translocation in PC12 cells. Nrf2 was marked using specific antibody (green) immunofluorescence. Nuclei were labeled using DAPI (blue). Typical photographs of merge and enlarge are shown. Scale bars represent 50 μm, the magnification of merge is 400×. (E) Down-regulation of Nrf2 expression with siRNA decreased the cytoprotective effect of **6**. Cells were transfected with 100 nM control siRNA (si-NC) or Nrf2 siRNA (si-Nrf2). The survival rates were determined by MTT assay. (F) Pretreatment with HO-1 inhibitor ZnPP (0.12 μM) suppressed the cytoprotective effect of **6**. PC12 cells were preincubated with **6** for 6 h prior to another 24 h of exposure to 500 μM H_2O_2. TBHQ (10 μM) was used as a positive control. Data are expressed as the mean ± SD, n = 3. $^{###}P < 0.001$, $^{##}P < 0.01$ vs control; $^{***}P < 0.001$, $^{**}P < 0.01$ vs H_2O_2; $^{\&\&\&}P < 0.001$ vs **6**+H_2O_2.

assay. In addition, **6** significantly promoted the nuclear translocation of Nrf2 as indicated by the strong green fluorescence observed in the nucleus in an immunofluorescence assay,[32,33] and the promotion effect of 5 μM **6** was comparable to that of the positive control TBHQ (Figure 5D). These findings confirmed that **6** is a potent activator of the Nrf2/ARE signaling in PC12 cells. Moreover, Nrf2 siRNA was applied to investigate if the antioxidant activity of **6** is dependent on Nrf2. Cell viability in the control siRNA group (si-NC) was increased by **6**, while the cytoprotection was reversed by the knockdown of Nrf2 (Figure 5E), which suggested that Nrf2 contributes to the antioxidant effect of **6**. This conclusion was further supported by the fact that cytoprotection of **6** was suppressed by the maximum noncytotoxic concentration of the HO-1 inhibitor zinc protoporphyrin (ZnPP) (Figure 5F). Thus, compound **6** exerted an antioxidant effect in PC12 cells involved activation of the Nrf2/ARE signaling and upregulated expression of HO-1.

The oxygen-glucose deprivation and reperfusion (OGD/R)-induced oxidative stress is the main pathological process of cerebral ischemia-reperfusion injury (CIRI).[3] Compound **6** was further evaluated for its neuroprotective effect against CIRI *in vitro* using the OGD/R-induced PC12 cell damage model. As shown in Figure S70, pretreatment with 5 μM **6** significantly reduced cell damage and the productions of LDH, MDA, and ROS. Its inhibitory activity against OGD/R-induced oxidative stress in PC12 cells is also related to the

https://doi.org/10.1021/acsomega.2c07891
ACS Omega 2023, 8, 8034−8044

Nrf2 pathway based on the fact that the cytoprotection was reversed by the knockdown of Nrf2 (Figure S70).

Finally, the neuroprotective effect of **6** against CIRI was evaluated using a rat model of transient middle artery occlusion (MCAO).[36,37] Compound **6** was preinjected into lateral ventricles 3 h after the ischemia-reperfusion injury. As shown in Figure 6, treatment with **6** (80 μg/kg) significantly reduced the size of brain infarction and neurological deficit score, implying potent neuroprotection against CIRI.

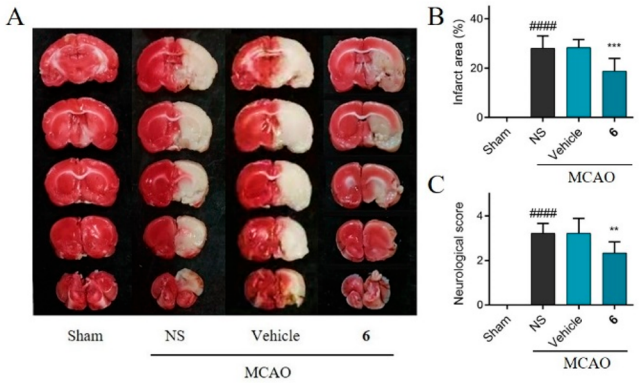

Figure 6. Protective effect of **6** against CIRI in a rat model of MCAO. (A) Representative images of triphenyl tetrazolium chloride (TTC)-stained brain slices of sham-operated (sham) rats and MCAO rats treated with normal saline (NS), vehicle (DMSO/NS, 1:100), and 80 μg/kg **6**. (B) Quantitative analysis of infarct size. (C) Neurological deficit score. Data are expressed as the mean ± SD, n = 6. $^{\#\#\#\#}P <$ 0.0001 vs sham-operated group; $^{***}P < 0.001$, $^{**}P < 0.01$ vs vehicle-treated group.

CONCLUSIONS

In summary, a further phytochemical investigation on the brown alga *D. coriacea* afforded five new xenicane diterpenes including three rare nitrogen-containing derivatives as the EtOH-adduct artifacts (**1**–**3**) and a rare xenicane with cyclobutanone moiety (**4**). All of the xenicanes (**1**–**20**) showed cytoprotective properties against H_2O_2-induced oxidative stress in PC12 cells. Compound **6** also had inhibitory activity against OGD/R-induced oxidative damage in PC12 cells. The antioxidant mechanism of **6** was suggested to be the activation of Nrf2/ARE signaling pathway. It is interesting to note that **6** showed significant neuroprotective effect against CIRI in a rat model of MCAO. This is the first report of neuroprotective properties of xenicane diterpenes against oxidative stress, providing evidence that xenicane might be a valuable lead scaffold for neuroprotective agents against CIRI.

EXPERIMENTAL SECTION

General Experimental Procedures. Optical rotations were measured with a PoLAAR 3005 digital polarimeter. UV and IR spectra were recorded with a TU 1901 spectrometer and an FTIR-850 spectrometer, respectively. ECD spectra were obtained with a Chirascan circular dichroism spectrometer. NMR spectra were acquired with Bruker Avance III NMR spectrometers running at 500 or 600 MHz for ^{1}H and 125 or 150 MHz for ^{13}C. Tetramethylsilane was used as an internal standard. (+)-HRESIMS data were recorded on a Thermo Scientific Q Exactive hybrid quadrupole-Orbitrap mass spectrometer. Column chromatography was performed with silica gel (200–300 mesh, Qingdao Marine Chemistry Co. Ltd.), ODS (50 μm, YMC), and Sephadex LH-20 (GE Healthcare Biosciences AB). High-performance liquid chromatography (HPLC) was performed using an Agilent 1100 series instrument equipped with a VWD G1314A detector and a YMC-Pack C_{18} column (10 μm, 250 × 10 mm).

Plant Material. Specimens of the brown alga *Dictyota coriacea* were collected off the coast of Nanji Island, Wenzhou, Zhejiang Province, China, in May 2018. The identification was carried out by one of the authors (Z.S.). A voucher specimen of the alga (ZN201801) was deposited at the Laboratory of Marine Natural Products Chemistry, Wenzhou Medical University, China.

Extraction and Isolation. The air-dried alga material (1.64 kg) was extracted with 95% EtOH at room temperature. The concentrated extract was partitioned between H_2O and EtOAc. Evaporation of EtOAc *in vacuo* afforded a dark residue of 130.5 g. The EtOAc fraction (100.2 g) was separated by silica gel vacuum column chromatography, eluting with a gradient of EtOAc/petroleum ether (1:15, 1:10, 1:4, and 1:2), to obtain five fractions (A–E). A portion of fraction C (2.0 g) was separated on a Sephadex LH-20 column, eluting with CH_2Cl_2/MeOH (1:1), to obtain three fractions (C1–C3). Fraction C2 (948.8 mg) was subjected to an ODS column, eluting with a stepwise gradient of MeOH/H_2O (65:35, 70:30, 75:25, 80:20, 85:15, and 90:10), to afford six fractions (C2a–C 2f). Fractions C2b (19.1 mg) was purified by C_{18} HPLC, using MeCN/H_2O (70:30) as eluent, to yield **4** (7.9 mg). Fraction C2c (86.7 mg) was purified by HPLC (MeCN/H_2O, 78:22) to obtain **1** (1.5 mg), **2** (4.5 mg), and **5** (1.6 mg). Fraction C 2d (154.2 mg) was separated by HPLC (MeCN/H_2O, 75:25) to yield **6** (80.8 mg) and **7** (28.4 mg). Fraction C2e (133.1 mg) was purified by HPLC (MeCN/H_2O, 80:20) to obtain **13** (6.7 mg). A portion of fraction D (3.1 g) was subjected to a Sephadex LH-20 column, eluting with CH_2Cl_2/MeOH (1:1), to afford three fractions (D1–D3). Fraction D2 (2.0 g) was further separated on an ODS column, eluting with a stepwise gradient of MeOH/H_2O (60:40, 65:35, 70:30, 75:25, 80:20, 85:15, and 90:10), to obtain 11 fractions (D2a–D2k). Fraction D2b (18.5 mg) was purified by HPLC (MeCN/H_2O, 60:40) to afford **20** (4.2 mg). Fraction D2c (349.5 mg) was separated by HPLC (MeCN/H_2O, 62:38) to yield **8** (16.0 mg), **10** (76.1 mg), and **15** (28.5 mg). Fraction D2d (432.2 mg) was purified by HPLC (MeCN/H_2O, 65:35) to obtain **14** (41.5 mg), **16** (20.0 mg), **17** (61.5 mg), and **19** (10.1 mg). Fractions D2e (29.0 mg) and D2f (134.3 mg) were purified by HPLC (MeCN/H_2O, 70:30) to yield **9** (4.7 mg) and **11** (20.4 mg), respectively. Compounds **3** (1.4 mg), **12** (2.5 mg), and **18** (2.4 mg) were separated from fraction D2i (56.1 mg) by HPLC using MeCN/H_2O (75:25) as eluent.

*Dictyolactam A (**1**).* Colorless oil; $[\alpha]^{25}$D, −124 (c 0.05, MeOH); UV (MeOH) λ_{max} (log ε) 221 (3.85) nm; ECD (MeOH) λ_{max} ($\Delta\varepsilon$) 217 (−59.26) nm; IR (KBr) ν_{max} 3273, 2972, 2920, 2861, 1697, 1451, 1383, 1088 cm^{-1}; ^{1}H and ^{13}C NMR data, Tables 1 and 2; HRESIMS m/z 412.2825 [M + Na]$^+$ (calcd for $C_{24}H_{39}NO_3Na$, 412.2822).

*Dictyolactam B (**2**).* Colorless oil; $[\alpha]^{25}$D −54 (c 0.05, MeOH); UV (MeOH) λ_{max} (log ε) 203 (4.18) nm; ECD (MeOH) λ_{max} ($\Delta\varepsilon$) 212 (−27.08) nm; IR (KBr) ν_{max} 3278, 2968, 2926, 2858, 1696, 1446, 1377, 1088 cm^{-1}; ^{1}H and ^{13}C NMR data, Tables 1 and 2; HRESIMS m/z 412.2804 [M + Na]$^+$ (calcd for $C_{24}H_{39}NO_3Na$, 412.2822).

https://doi.org/10.1021/acsomega.2c07891
ACS Omega 2023, 8, 8034–8044

*9-Demethoxy-9-ethoxyjoalin (**3**).* Colorless oil; $[\alpha]^{25}$D +12 (*c* 0.05, MeOH); UV (MeOH) λ_{max} (log ε) 203 (4.07) nm; ECD (MeOH) λ_{max} ($\Delta\varepsilon$) 254 (+17.94), 208 (−62.29) nm; IR (KBr) 3346, 2970, 2929, 1708, 1446, 1379, 1267, 1090, 982, 735, 636 cm^{-1}; ^{1}H and ^{13}C NMR data, Tables 1 and 2; HRESIMS *m*/*z* 382.2339 $[M + Na]^+$ (calcd for $C_{22}H_{33}NO_3Na$, 382.2353).

*4-Hydroxyisoacetylcoriacenone (**4**).* Colorless oil; $[\alpha]^{25}$D −78 (*c* 0.05, MeOH); IR (KBr) ν_{max} 3514, 2926, 2860, 1758, 1664, 1606, 1446, 1375, 1227, 1020 cm^{-1}; UV (MeOH) λ_{max} (log ε) 230 (3.80) nm; ECD (MeOH) λ_{max} ($\Delta\varepsilon$) 315 (−6.99), 238 (+52.50), 210 (−47.37) nm; ^{1}H and ^{13}C NMR data, Tables 1 and 2; HRESIMS *m*/*z* 383.2175 $[M + Na]^+$ (calcd for $C_{22}H_{32}O_4Na$, 383.2193).

*19-O-Acetyldictyodiol (**5**).* Colorless oil; $[\alpha]^{25}$D +56 (*c* 0.05, MeOH); IR (KBr) ν_{max} 3458, 2925, 2854, 1734, 1664, 1587, 1446, 1377, 1234, 1026 cm^{-1}; ^{1}H and ^{13}C NMR data, Tables 1 and 2; HRESIMS *m*/*z* 371.2541 $[M + Na]^+$ (calcd for $C_{22}H_{36}O_3Na$, 371.2557).

ECD Calculation. All density functional theory (DFT) calculations were performed using Gaussian 16 (G16).[38] Conformers of molecules **1**−**4** were obtained using the GMMX package implemented in GaussView 6.0 with the MMFF94 force field. A total of 114, 168, 268, and 102 conformers were yielded for **1**−**4**, respectively, with an energy window of 3.5 kcal/mol. The conformational energy plots for **1**−**4** were shown in Figures S71−S74. In addition, 11 lower-energy conformers of **1**−**4** were further optimized at different levels of theory. The semiempirical calculation PM6 in the G16 was used for structure optimization in MeOH with the polarizable continuum model (PCM). Conformers of **1**−**4** were fully optimized at the CAM-B3LYP/6-311G(2d,p) level. The vibrational frequencies analysis showed no imaginary frequency, and the locally stable structure was obtained. Then the ECD calculations were carried out at the B3LYP/Def2-TZVP level using the time-dependent DFT theory (TD-DFT), in which 30 singlet excited states were investigated to obtain the ECD data of each conformer. Moreover, the electronic spectra of mixture in GaussView 6.0 was applied to analyze the Gibbs free energy and Boltzmann distribution for the 11 lower-energy conformers of **1**−**4** (Table S1). The dominant conformations (No. 7 for **1**; 11 and 7 for **2**; 1, 4, 10, and 3 for **3**; 8, 2, and 1 for **4**) were computed to generate the weighted ECD curves for **1**−**4**.

Cell Culture, MTT Assay, Colony Formation Assay, Western Blot Analysis, and Transfection Assay. The previously reported protocols[32,33] were followed except that the treatment time and concentration of H_2O_2 were modified as indicated in the figure captions.

Detections of LDH, MDA, GSH, GSH-Px, and SOD. PC12 cells in logarithmic growth phase were cultured in six-well plates at a density of 5×10^5 cells/mL and underwent various treatments. The supernatant was collected for LDH assay and the cells were collected for MDA, GSH, GSH-Px, and SOD assays following the manufacturer's instructions for assay kits (Nanjing Jiancheng Bioengineering Institute).

DPPH Radical Scavenging Assay. The ethanol solutions of **6** (2.5, 5, 10, and 20 μM) were mixed with 0.15 mM DPPH in ethanol in a 96-well plate. The absorbances of the reaction mixtures were recorded at 517 nm using a microplate reader after the plate was stored at 25 °C in the dark for 30 min. TBHQ (20 μM) was used as a positive control.

Intracellular ROS Analysis. PC12 cells were cultured in six-well plates at a density of 5×10^5 cells/mL. Each well was incubated with 1 mL DCFH-DA (the final concentration was 10 μM) for 20 min. Cells were washed three times with medium and followed by drug treatments. Subsequently, the ROS level was quantified using a flow cytometry (Becton, Dickinson and Company) and analyzed with FlowJo software.

Immunostaining of Nrf2. A previously reported protocol[32,33] was followed except that the secondary antibody was replaced by goat antirabbit IgG (ab150077, Abcam).

OGD/R-Treatment. The PC12 cells were cultured in DMEM for 24 h and washed with PBS for three times. The medium was then replaced by a glucose-free DMEM and the cells were transferred to an incubator with 1% O_2, 5% CO_2, and 94% N_2 at 37 °C. After 10 h, the medium was changed back to high-glucose DMEM. The cells were cultured in a normal incubator humidified with 5% CO_2 balanced with air at 37 °C for 24 h of recovery time. A control group was also run in which PC12 cells were cultured in DMEM and left untreated.

Experimental Animals. Adult male Sprague−Dawley (SD) rats (250−280 g) were obtained from the Beijing Vital River Laboratory Animal Technology Co., Ltd. The rats were raised under a 12/12 h dark/light cycle and had free access to adequate food and sterile water. The indoor temperature was controlled at around 24 °C and the relative humidity was set as 40%−50%. Animals were adapted for 1 week before starting the experiments. All animal procedures were approved by the Animal Welfare Committee of Wenzhou Medical University (Protocol No.:WYDW2019−0419).

CIRI Based on MCAO Model, Intracerebroventricular Injection, Neurological Deficit Score, and TTC Staining. The previously reported protocols[31,33] were followed except that the drugs were injected 3 h after reperfusion and the neurological deficit score and brain infarct size by TTC staining were evaluated 24 h after drug treatment.

Statistical Analysis. Experimental data were expressed as mean ± standard deviation (SEMs). SPSS 20.0 software was used for statistical analysis. The statistical significance was analyzed by using a Student's *t* test or one-way ANOVA for multiple comparisons. *P* values less than 0.05 were considered as statistically significant.

■ ASSOCIATED CONTENT

Supporting Information

The Supporting Information is available free of charge at https://pubs.acs.org/doi/10.1021/acsomega.2c07891.

1D and 2D NMR and HRESIMS spectra of the new compounds **1**−**5**, NMR spectra of the known compounds **6**−**20**, ECD and calculated ECD spectra for **1**−**4**, details for the ECD calculation, the cytotoxicity against PC12 cells, DPPH radical scavenging effect, and inhibition against OGD/R-induced oxidative damage of **6** (PDF)

■ AUTHOR INFORMATION

Corresponding Authors

Pengcheng Yan − *School of Pharmaceutical Sciences, Wenzhou Medical University, Wenzhou, Zhejiang 325035, People's Republic of China;* orcid.org/0000-0002-9114-2244; Email: yanpc@wmu.edu.cn

https://doi.org/10.1021/acsomega.2c07891
ACS Omega 2023, 8, 8034−8044

Jianzhang Wu − *The Eye Hospital, School of Ophthalmology & Optometry, Wenzhou Medical University, Wenzhou 325027, People's Republic of China; Oujiang Laboratory (Zhejiang Lab for Regenerative Medicine, Vision and Brain Health), Wenzhou, Zhejiang 325000, People's Republic of China; School of Pharmaceutical Sciences, Wenzhou Medical University, Wenzhou, Zhejiang 325035, People's Republic of China;* orcid.org/0000-0002-2782-745X; Email: wjzwzmu@163.com

Authors

Yu Qi − *School of Pharmaceutical Sciences, Wenzhou Medical University, Wenzhou, Zhejiang 325035, People's Republic of China*

Ge Liu − *School of Pharmaceutical Sciences, Wenzhou Medical University, Wenzhou, Zhejiang 325035, People's Republic of China*

Chengyan Fang − *Department of Pharmacy, Shaoxing Hospital of Traditional Chinese Medicine, Shaoxing, Zhejiang 312000, People's Republic of China*

Chengcheng Jing − *School of Pharmaceutical Sciences, Wenzhou Medical University, Wenzhou, Zhejiang 325035, People's Republic of China*

Shuhua Tang − *School of Pharmaceutical Sciences, Wenzhou Medical University, Wenzhou, Zhejiang 325035, People's Republic of China*

Ge Li − *School of Pharmaceutical Sciences, Wenzhou Medical University, Wenzhou, Zhejiang 325035, People's Republic of China*

Chaojie Wang − *School of Pharmaceutical Sciences, Wenzhou Medical University, Wenzhou, Zhejiang 325035, People's Republic of China*

Haoru Zhu − *School of Pharmaceutical Sciences, Wenzhou Medical University, Wenzhou, Zhejiang 325035, People's Republic of China*

Min Zhao − *School of Pharmaceutical Sciences, Wenzhou Medical University, Wenzhou, Zhejiang 325035, People's Republic of China*

Zhongmin Sun − *Institute of Oceanology, Chinese Academy of Sciences, Qingdao 266071, People's Republic of China*

Complete contact information is available at: https://pubs.acs.org/10.1021/acsomega.2c07891

Author Contributions

▽Y. Qi, G. Liu, and C. Fang made equal contributions to this work.

Notes

The authors declare no competing financial interest.

■ ACKNOWLEDGMENTS

This work was financially supported by the National Natural Science Foundation of China (Grant No. 82073761), the Natural Science Foundation of Zhejiang Province, China (Grant No. LQ19H300003), and the Outstanding Youth Foundation from Wenzhou Medical University (Grant No. 604091809). We thank the Scientific Center of Wenzhou Medical University for consultation and instrument availability that supported this work.

■ REFERENCES

(1) Ma, H.; Campbell, B. C. V.; Parsons, M. W.; Churilov, L.; Levi, C. R.; Hsu, C.; Kleinig, T. J.; Wijeratne, T.; Curtze, S.; Dewey, H. M.; Miteff, F.; Tsai, C. H.; Lee, J. T.; Phan, T. G.; Mahant, N.; Sun, M. C.; Krause, M.; Sturm, J.; Grimley, R.; Chen, C. H.; Hu, C. J.; Wong, A. A.; Field, D.; Sun, Y.; Barber, P. A.; Sabet, A.; Jannes, J.; Jeng, J. S.; Clissold, B.; Markus, R.; Lin, C. H.; Lien, L. M.; Bladin, C. F.; Christensen, S.; Yassi, N.; Sharma, G.; Bivard, A.; Desmond, P. M.; Yan, B.; Mitchell, P. J.; Thijs, V.; Carey, L.; Meretoja, A.; Davis, S. M.; Donnan, G. A. Thrombolysis guided by perfusion imaging up to 9 h after onset of stroke. *N. Engl. J. Med.* **2019**, *380*, 1795−1803.

(2) Li, Q.; Xing, S.; Chen, Y.; Liao, Q.; Li, Q.; Liu, Y.; He, S.; Feng, F.; Chen, Y.; Zhang, J.; Liu, W.; Guo, Q.; Sun, Y.; Sun, H. Reasonably activating Nrf2: A long-term, effective and controllable strategy for neurodegenerative diseases. *Eur. J. Med. Chem.* **2020**, *185*, 111862.

(3) Wu, G.; Zhu, L.; Yuan, X.; Chen, H.; Xiong, R.; Zhang, S.; Cheng, H.; Shen, Y.; An, H.; Li, T.; Li, H.; Zhang, W. Britanin ameliorates cerebral ischemia-reperfusion injury by inducing the Nrf2 protective pathway. *Antioxid. Redox. Signal.* **2017**, *27*, 754−768.

(4) Wang, H.; Wei, W.; Lan, X.; Liu, N.; Li, Y.; Ma, H.; Sun, T.; Peng, X.; Zhuang, C.; Yu, J. Neuroprotective effect of swertiamain on cerebral ischemia/reperfusion injury by inducing the Nrf2 protective pathway. *ACS Chem. Neurosci.* **2019**, *10*, 2276−2286.

(5) Gao, Y.; Hu, M.; Niu, X.; Li, M.; Xu, L.; Xiao, Y.; Zhang, J.; Wang, H.; Li, L.; Chu, B.; Lv, P. Dl-3-n-Butylphthalide improves neuroinflammation in mice with repeated cerebral ischemia-reperfusion injury through the Nrf2-mediated antioxidant response and TLR4/MyD88/NF-κB signaling pathway. *Oxid. Med. Cell. Longev.* **2022**, *2022*, 8652741.

(6) Wu, J.; Xi, Y.; Li, G.; Zheng, Y.; Wang, Z.; Wang, J.; Fang, C.; Sun, Z.; Hu, L.; Jiang, W.; Dai, L.; Dong, J.; Qiu, P.; Zhao, M.; Yan, P. Hydroazulene diterpenes from a *Dictyota* brown alga and their antioxidant and neuroprotective effects against cerebral ischemia-reperfusion injury. *J. Nat. Prod.* **2021**, *84*, 1306−1315.

(7) Chen, J.; Li, H.; Zhao, Z.; Xia, X.; Li, B.; Zhang, J.; Yan, X. Diterpenes from the marine algae of the genus *Dictyota*. *Mar. Drugs* **2018**, *16*, 159.

(8) Viano, Y.; Bonhomme, D.; Camps, M.; Briand, J. F.; Ortalo-Magne, A.; Blache, Y.; Piovetti, L.; Culioli, G. Diterpenoids from the Mediterranean brown alga *Dictyota* sp. evaluated as antifouling substances against a marine bacterial biofilm. *J. Nat. Prod.* **2009**, *72*, 1299−1304.

(9) Ayyad, S. E. N.; Makki, M. S.; Al-Kayal, N. S.; Basaif, S. A.; El-Foty, K. O.; Asiri, A. M.; Alarif, W. M.; Badria, F. A. Cytotoxic and protective DNA damage of three new diterpenoids from the brown alga *Dictyota dichotoma*. *Eur. J. Med. Chem.* **2011**, *46*, 175−182.

(10) Tringali, C.; Oriente, G.; Piattelli, M.; Nicolosi, G. Two minor dolabellane diterpenoid constituents from a *Dictyota* Species. *J. Nat. Prod.* **1985**, *48*, 484−485.

(11) Pereira, H. S.; Leão-Ferreira, L. R.; Moussatché, N.; Teixeira, V. L.; Cavalcanti, D. N.; Costa, L. J.; Diaz, R.; Frugulhetti, I. C. P. P. Antiviral activity of diterpenes isolated from the Brazilian marine alga *Dictyota menstrualis* against human immunodeficiency virus type 1 (HIV-1). *Antivir. Res.* **2004**, *64*, 69−76.

(12) Cheng, S.; Zhao, M.; Sun, Z.; Yuan, W.; Zhang, S.; Xiang, Z.; Cai, Y.; Dong, J.; Huang, K.; Yan, P. Diterpenes from a Chinese collection of the brown alga *Dictyota plectens*. *J. Nat. Prod.* **2014**, *77*, 2685−2693.

(13) Zhao, M.; Cheng, S.; Yuan, W.; Dong, J.; Huang, K.; Sun, Z.; Yan, P. Further new xenicanes from a Chinese collection of the brown alga *Dictyota plectens*. *Chem. Pharm. Bull.* **2015**, *63*, 1081−1086.

(14) Abrantes, J. L.; Barbosa, J.; Cavalcanti, D.; Pereira, R. C.; Frederico Fontes, C. L.; Teixeira, V. L.; Moreno Souza, T. L.; Paixão, I. C. P. The effects of the diterpenes isolated from the Brazilian brown algae *Dictyota pfaffii* and *Dictyota menstrualis* against the herpes simplex type-1 replicative cycle. *Planta Med.* **2010**, *76*, 339−344.

(15) Yan, P.; Li, G.; Wang, C.; Wu, J.; Sun, Z.; Martin, G. E.; Wang, X.; Reibarkh, M.; Saurí, J.; Gustafson, K. R. Characterization by empirical and computational methods of dictyospiromide, an intriguing antioxidant alkaloid from the marine alga *Dictyota coriacea*. *Org. Lett.* **2019**, *21*, 7577−7581.

(16) Norte, M.; González, A. G.; Arroyo, P.; Zárraga, M.; Pérez, C.; Rodriguez, M. L.; Ruiz-Perez, C.; Dorta, L. New xenicane diterpenes

from the brown algae of Dictyotaceae. *Tetrahedron* **1990**, *46*, 6125−6132.
(17) Enoki, N.; Ishida, R.; Matsumoto, T. Structures and conformations of new nine-membered ring diterpenoids from the marine alga *Dictyota dichotoma*. *Chem. Lett.* **1982**, *11*, 1749−1752.
(18) Guella, G.; Chiasera, G.; N'Diaye, I.; Pietra, F. Xenicane diterpenes revisited: Thermal (E)→(Z) isomerization and conformational motions. A unifying picture. *Helv. Chim. Acta* **1994**, *77*, 1203−1221.
(19) Othmani, A.; Bouzidi, N.; Viano, Y.; Alliche, Z.; Seridi, H.; Blache, Y.; El Hattab, M.; Briand, J.-F.; Culioli, G. Anti-microfouling properties of compounds isolated from several Mediterranean *Dictyota* spp. *J. Appl. Phycol.* **2014**, *26*, 1573−1584.
(20) Ovenden, S. P.; Nielson, J. L.; Liptrot, C. H.; Willis, R. H.; Tapiolas, D. M.; Wright, A. D.; Motti, C. A. Update of spectroscopic data for 4-hydroxydictyolactone and dictyol E isolated from a *Halimeda stuposa-Dictyota* sp. assemblage. *Molecules* **2012**, *17*, 2929−2938.
(21) Sun, H. H.; McEnroe, F. J.; Fenical, W. Acetoxycrenulide, a new bicyclic cyclopropane-containing diterpenoid from the brown seaweed *Dictyota crenulata*. *J. Org. Chem.* **1983**, *48*, 1903−1906.
(22) Midland, S. L.; Wing, R. M.; Sims, J. J. New crenulides from the sea hare. *Aplysia vaccaria*. *J. Org. Chem.* **1983**, *48*, 1906−1909.
(23) Kusumi, T.; Muanza-Nkongolo, D.; Goya, M.; Ishitsuka, M.; Iwashita, T.; Kakisawa, H. Structures of crenulacetals A, B, C, and D. The new diterpenoids from the brown algae of Dictyotaceae. *J. Org. Chem.* **1986**, *51*, 384−387.
(24) Ishitsuka, M.; Kusumi, T.; Kakisawa, H.; Enoki, N.; Matsumoto, T. Biomimetic cyclization of dictyodiacetal: The stereochemistry of fukurinal. *J. Nat. Prod.* **1985**, *48*, 477−479.
(25) Coates, R. M.; Ley, D. A.; Cavender, P. L. Synthesis and carbon-13 nuclear magnetic resonance spectra of all-*trans*-geranylgeraniol and its nor analogs. *J. Org. Chem.* **1978**, *43*, 4915−4922.
(26) Couperus, P. A.; Clague, A. D. H.; van Dongen, J. P. C. M. ^{13}C chemical shifts of some model olefins. *Org. Magn. Reson.* **1976**, *8*, 426−431.
(27) Uchida, I.; Kuriyama, K. The π-π circular dichroism of $\delta\beta$-unsaturated γ-lactones. *Tetrahedron Lett.* **1974**, *15*, 3761−3764.
(28) Guella, G.; N'Diaye, I.; Chiasera, G.; Pietra, F. Joalin, the first nitrogen-containing xenicane diterpene isolated from a brown seaweed collected off the Senegalese coast. *J. Chem. Soc. Perk. Trans. 1* **1993**, No. 14, 1545−1546.
(29) Ishitsuka, M.; Kusumi, T.; Kakisawa, H.; Kawakami, Y.; Nagai, Y.; Sato, T. Novel diterpenes with a cyclobutenone moiety from the brown alga, *Pachydictyon coriaceum*. *J. Org. Chem.* **1983**, *48*, 1937−1938.
(30) Finer, J.; Clardy, J.; Fenical, W.; Minale, L.; Riccio, R.; Battaile, J.; Kirkup, M.; Moore, R. E. Structures of dictyodial and dictyolactone, unusual marine diterpenoids. *J. Org. Chem.* **1979**, *44*, 2044−2047.
(31) Huang, L.; Wang, J.; Chen, L.; Zhu, M.; Wu, S.; Chu, S.; Zheng, Y.; Fan, Z.; Zhang, J.; Li, W.; Chen, D.; Yang, X.; Wang, S.; Qiu, P.; Wu, J. Design, synthesis, and evaluation of NDGA analogues as potential anti-ischemic stroke agents. *Eur. J. Med. Chem.* **2018**, *143*, 1165−1173.
(32) Wu, J.; Xi, Y.; Huang, L.; Li, G.; Mao, Q.; Fang, C.; Shan, T.; Jiang, W.; Zhao, M.; He, W.; Dong, J.; Li, X.; Qiu, P.; Yan, P. A steroid-type antioxidant targeting the Keap1/Nrf2/ARE signaling pathway from the soft coral *Dendronephthya gigantea*. *J. Nat. Prod.* **2018**, *81*, 2567−2575.
(33) Li, G.; Zheng, Y.; Yao, J.; Hu, L.; Liu, Q.; Ke, F.; Feng, W.; Zhao, Y.; Yan, P.; He, W.; Deng, H.; Qiu, P.; Li, W.; Wu, J. Design and green synthesis of piperlongumine analogs and their antioxidant activity against cerebral ischemia-reperfusion injury. *ACS Chem. Neurosci.* **2019**, *10*, 4545−4557.
(34) Ma, S.; Liu, H.; Jiao, H.; Wang, L.; Chen, L.; Liang, J.; Zhao, M.; Zhang, X. Neuroprotective effect of ginkgolide K on glutamate-induced cytotoxicity in PC 12 cells via inhibition of ROS generation and Ca^{2+} influx. *Neurotoxicology* **2012**, *33*, 59−69.
(35) Jung, K. A.; Kwak, M. K. The Nrf2 system as a potential target for the development of indirect antioxidants. *Molecules* **2010**, *15*, 7266−7291.
(36) Gubskiy, I. L.; Namestnikova, D. D.; Cherkashova, E. A.; Chekhonin, V. P.; Baklaushev, V. P.; Gubsky, L. V.; Yarygin, K. N. MRI guiding of the middle cerebral artery occlusion in rats aimed to improve stroke modeling. *Transl. Stroke Res.* **2018**, *9*, 417−425.
(37) Rosell, A.; Agin, V.; Rahman, M.; Morancho, A.; Ali, C.; Koistinaho, J.; Wang, X. Y.; Vivien, D.; Schwaninger, M.; Montaner, J. Distal occlusion of the middle cerebral artery in mice: Are we ready to assess long-term functional outcome? *Transl. Stroke Res.* **2013**, *4*, 297−307.
(38) Frisch, M. J.; Trucks, G. W.; Schlegel, H. B.; Scuseria, G. E.; Robb, M. A.; Cheeseman, J. R.; Scalmani, G.; Barone, V.; Petersson, G. A.; Nakatsuji, H.; Li, X.; Caricato, M.; Marenich, A. V.; Bloino, J.; Janesko, B. G.; Gomperts, R.; Mennucci, B.; Hratchian, H. P.; Ortiz, J. V.; Izmaylov, A. F.; Sonnenberg, J. L.; Williams-Young, D.; Ding, F.; Lipparini, F.; Egidi, F.; Goings, J.; Peng, B.; Petrone, A.; Henderson, T.; Ranasinghe, D.; Zakrzewski, V. G.; Gao, J.; Rega, N.; Zheng, G.; Liang, W.; Hada, M.; Ehara, M.; Toyota, K.; Fukuda, R.; Hasegawa, J.; Ishida, M.; Nakajima, T.; Honda, Y.; Kitao, O.; Nakai, H.; Vreven, T.; Throssell, K.; Montgomery, J. A., Jr.; Peralta, J. E.; Ogliaro, F.; Bearpark, M. J.; Heyd, J. J.; Brothers, E. N.; Kudin, K. N.; Staroverov, V. N.; Keith, T. A.; Kobayashi, R.; Normand, J.; Raghavachari, K.; Rendell, A. P.; Burant, J. C.; Iyengar, S. S.; Tomasi, J.; Cossi, M.; Millam, J. M.; Klene, M.; Adamo, C.; Cammi, R.; Ochterski, J. W.; Martin, R. L.; Morokuma, K.; Farkas, O.; Foresman, J. B.; Fox, D. J. *Gaussian 16, Revision A.03*; Gaussian, Inc.: Wallingford, CT, 2016.

https://doi.org/10.1021/acsomega.2c07891
ACS Omega 2023, 8, 8034−8044